Molecular Biology of the Cell
Vol. 19, 3625–3637, September 2008

Different Domains of the UBL-UBA Ubiquitin Receptor, Ddi1/Vsm1, Are Involved in Its Multiple Cellular Roles

Galina Gabriely, Rachel Kama, Rita Gelin-Licht, and Jeffrey E. Gerst

Department of Molecular Genetics, Weizmann Institute of Science, Rehovot 76100, Israel

Submitted May 18, 2007; Revised June 4, 2008; Accepted June 6, 2008
Monitoring Editor: Akihiko Nakano

Ddi1/Vsm1 is an ubiquitin receptor involved in regulation of the cell cycle and late secretory pathway in *Saccharomyces cerevisiae*. Ddi1 possesses three domains: an NH_2-terminal ubiquitin-like domain (UBL), a COOH-terminal ubiquitin-associated domain (UBA), and a retroviral aspartyl-protease domain (RVP). Here, we demonstrate the domains involved in homodimerization, checkpoint regulation, localization, and t-SNARE binding. The RVP domain is required for protein homodimerization, whereas the UBL and UBA domains are required for rescue of the *pds1-128* checkpoint mutant and enrichment of GFP-Ddi1 in the nucleus. A mutation in aspartate-220, which is necessary for putative aspartyl-protease function, abolished the rescue of *pds1-128* cells but not homodimerization. Thus, Ddi1 catalytic activity may be required for checkpoint regulation. The Sso1 t-SNARE-interacting domain maps to residues 344–395 and undergoes phosphorylation on threonines T346 and T348. T348 is necessary for Sso binding, and phosphorylation is important for function, because mutations that lessen phosphorylation (e.g., Ddi1^{T346A}, Ddi1^{T348A}) are unable to facilitate growth of the *sec9-4* t-SNARE mutant. In contrast, the overproduction of phosphorylatable forms of Ddi1 (e.g., Ddi1, Ddi1^{S341A}) rescue the growth of *sec9-4* cells similar to Sso1 overproduction. Thus, Ddi1 participates in multiple cellular processes via its different domains and phosphorylation may regulate exocytic functions.

INTRODUCTION

DDI1 (DNA Damage-Inducible 1) was initially found as a gene induced transcriptionally in response to a variety of genotoxic stresses in yeast (Liu and Xiao, 1997), although a direct role for the Ddi1 protein in DNA repair has not been established. Ddi1 is composed of at least three domains: an amino-terminal ubiquitin-like domain (UBL), a carboxy-terminal ubiquitin-associated domain (UBA), and an aspartyl protease domain conserved from retroviruses (RVP), which is positioned between the UBL and UBA domains. The UBL domain of Ddi1 shares 16% identity with ubiquitin (Bertolaet *et al.*, 2001b) and was shown to bind to the proteasome (Kaplun *et al.*, 2005); the UBA domain, on the other hand, interacts with ubiquitylated cargoes (e.g., HO endonuclease; Kaplun *et al.*, 2005; Ivantsiv *et al.*, 2006). Therefore, Ddi1, together with other UBL- and UBA-bearing proteins in *Saccharomyces cerevisiae* (namely, Rad23 and Dsk2), were classified as UBL-UBA ubiquitin receptors that mediate proteasomal degradation of ubiquitylated cargoes (Lambertson *et al.*, 1999; Clarke *et al.*, 2001; Hartmann-Petersen and Gordon, 2004; Elsasser and Finley, 2005; Hicke *et al.*, 2005). Interestingly, Rad23 forms heterodimers with Ddi1 or Dsk2, and Ddi1 binding to Rad23 is mediated by interactions between their UBL and UBA domains (Rao and Sastry, 2002; Kang *et al.*, 2006).

In addition to heterodimerization, all three UBL-UBA ubiquitin receptors in *S. cerevisiae* appear to undergo homodimerization, whose biological role remains unknown. Rad23 and Dsk2 homodimerize through their UBA domains (Bertolaet *et al.*, 2001a; Sasaki *et al.*, 2005), whereas Ddi1 requires neither the UBA nor UBL domains for dimerization (Bertolaet *et al.*, 2001a). Additionally, it was shown that the UBA domains of Rad23 and Ddi1 are able to noncovalently bind single ubiquitin molecules (Bertolaet *et al.*, 2001b) and multiubiquitin chains (Wilkinson *et al.*, 2001; Kang *et al.*, 2006). Moreover, K48-linked tetraubiquitin can interact simultaneously with the UBA domains of Rad23 and Ddi1, although the Rad23-Ddi1 heterodimer has to undergo dissociation before tetraubiquitin binding (Kang *et al.*, 2006). By employing such a mechanism, the UBL-UBA ubiquitin receptors are thought to prevent unnecessary ubiquitin-chain elongation or deubiquitylation during the transit of substrates to the proteasome (Kang *et al.*, 2006). For instance, Clarke and coworkers (Bertolaet *et al.*, 2001b) suggested that the UBA domains of Rad23 and Ddi1 are able to recognize ubiquitylated Pds1, a checkpoint factor involved in regulating sister chromatid separation, and thereby inhibit the ubiquitin chain elongation required for targeting Pds1 to the 26S proteasome. Overproduction of either Ddi1 or Rad23 rescues the temperature sensitivity of a mutant *PDS1* allele (*pds1-128*), suggesting a role for these proteins in Pds1-dependent S-phase checkpoint control (Clarke *et al.*, 2001). Recent studies show that the UBA domain of Ddi1 is also involved in the interaction with the Ufo1 E3 enzyme and its target, HO endonuclease, an initiator of a mating-type switching (Kaplun *et al.*, 2005; Ivantsiv *et al.*, 2006), which is stabilized in the absence of Ddi1 (Kaplun *et al.*, 2005).

This article was published online ahead of print in *MBC in Press* (http://www.molbiolcell.org/cgi/doi/10.1091/mbc.E07–05–0462) on June 18, 2008.

Address correspondence to: Jeffrey E. Gerst (jeffrey.gerst@weizmann.ac.il).

Abbreviations used: Ddi1, DNA damage inducible 1; GFP, green fluorescent protein; HIV, human immunodeficiency virus; IP, immunoprecipitation; MS, mass spectrometry; Pds1, Precocious Dissociation of Sisters; RVP, retroviral aspartyl protease domain; SNARE, soluble *N*-ethylmaleimide-sensitive fusion protein attachment protein receptor; UBA, ubiquitin-associated domain; UBL, ubiquitin-like domain; WT, wild type; vps, vacuolar protein sorting.

A unique feature of Ddi1 among the UBL-UBA ubiquitin receptors is the presence of an evolutionary conserved RVP domain (Krylov and Koonin, 2001; Sirkis *et al.*, 2006), whose functional catalytic activity has not been established yet. The D[ST]G (aspartate-serine/threonine-glycine) signature of this motif, which is hallmark of aspartyl proteases, is conserved between Ddi1 orthologues up to mammals (Krylov and Koonin, 2001). All structurally characterized aspartyl proteases form bilobed structures with the two catalytic aspartates located between the lobes that hold the activated water molecule necessary for peptide bond hydrolysis (Davies, 1990). In retroviral proteases, the two lobes are supplied by identical domains that form a homodimer. Human immunodeficiency viruses (HIVs) utilize an aspartyl protease for the maturational processing of their *gag* and *pol* polyproteins. However, in Ddi1 the biological role and necessity of the protease domain is still not understood. Recently, the crystal structure of the RVP domain of Ddi1 in its homodimerized state was resolved (Sirkis *et al.*, 2006), demonstrating remarkable similarity to the dimer fold of retroviral proteases. Moreover, the active sites of both HIV protease and Ddi1 share the same DTGA tetrapeptide (aspartate-threonine-glycine-alanine) that preserves the geometrical identity in their structures. This supports the idea that Ddi1 may play a proteolytic role in yeast.

Ddi1-related aspartyl proteases are conserved in evolution (Krylov and Koonin, 2001) and include human homologues, like Ddi1 and Ddi2, and neuron-specific nuclear receptors, NIX1, NRIP2, and NRIP3. Recently, a novel retroviral-like aspartyl protease called skin aspartic protease (SASPase), which possesses autocatalytic activity and is expressed specifically in epidermis, was identified in humans (hSASP; Bernard *et al.*, 2005). A later study showed that the mouse homologue of SASPase (mSASP) is involved in prevention of fine wrinkle formation (Matsui *et al.*, 2006). Thus, this novel class of retroviral-like aspartyl proteases may play a role in the physiology of mammalian tissue architecture (Matsui *et al.*, 2006).

Ddi1 was isolated in our laboratory from a two-hybrid screen using the v-SNARE (soluble *N*-ethylmaleimide-sensitive fusion protein attachment protein receptor), Snc2, as the bait protein (Lustgarten and Gerst, 1999). Binding studies demonstrated that Ddi1 interacts with both the Snc1 and Snc2 exo- and endocytic v-SNAREs, although the binding activity toward Snc2 is higher than for Snc1. Overexpression of *DDI1* in yeast bearing a mutation in Sec9 t-SNARE (*sec9-4*) inhibits secretion and cell growth, and results in the accumulation of low-density secretory vesicles. On the basis of these observations, it was proposed that Ddi1 functions as a negative regulator of exocytosis in yeast. More recently, our laboratory demonstrated the direct interaction of Ddi1 with the exocytic t-SNARE, Sso1, in a phosphorylation-dependent manner (Marash and Gerst, 2003). The binding of Sso1 to Ddi1 prevents the association of Sso1 with its cognate t-SNARE partner, Sec9, which also points toward an inhibitory role for Ddi1 in regulating late exocytic processes. Importantly, the UBA domain of Ddi1 is not required for this interaction.

The abovementioned observations indicate that Ddi1 is likely to be involved in multiple cellular processes connected to growth control. To better characterize the diverse biological roles filled by Ddi1, we used mutational analysis to show the requirements of the different domains for its various ascribed functions. We demonstrate that the RVP domain is required for the homodimerization of Ddi1 in vivo. In contrast, the UBL and UBA domains are required for both the enrichment of GFP-Ddi1 in the nucleus and for suppression of the *pds1-128* mutant. This suggests a connection between the nuclear localization of Ddi1 and possible stabilization of the mutant Pds1 protein. Interestingly, the aspartyl protease motif is also necessary for the rescue of *pds 1-128* cells at restrictive temperatures, indicating that Ddi1 must be catalytically active to rescue the Pds 1-128 defect. Finally, we show that amino acids 344–395 mediate Ddi1 binding to the Sso1 t-SNARE and that this interaction domain is modified posttranslationally by phosphorylation on specific threonine residues, which is important for function in vivo. In conclusion, we show that different domains of Ddi1 are involved in its diverse functions.

Table 1. Yeast strains used in this study

Name	Genotype	Source
W303-1a (WT)	*MAT*a *can1 his3 leu2 lys2 trp1 ura3 ade2*	J. Hirsch
BY 4741 (WT)	*MAT*a *his3Δ1 leuΔ0 met15Δ0 ura3Δ0*	Euroscarf
DCY1167 (*pds1-128*)	*MATα leu2 pds1-128*	S. Reed
VL2 (*ddi1Δ*)	*MAT*a *his3 leu2 trp1 ade2 ddi1Δ::URA3*	J. Gerst
Y06141 (*ddi1Δ*)	*MAT*a *his3Δ1 leuΔ0 met15Δ0 ura3Δ0 ddi1Δ::kanMX*	Euroscarf
ATCC[a] 201389 (*SIK1-RFP*)	*MATα his3Δ1 leu2Δ0 lys2Δ0 ura3Δ0 SIK1-RFP::kanMX*	J. Falvo (University of California, San Francisco)
NY782 (*sec9-4*)	*MAT*a *leu2-3,112 ura3-52 sec9-4*	P. Novick
GGY12 (*GAL-GFP-DDI1*)	*MAT*a *his3Δ1 leuΔ0 met15Δ0 ura3Δ0 GAL1-GFP-DDI1::HIS3*	This study

[a] ATCC, American Type Culture Collection.

MATERIALS AND METHODS

Yeast Strains and Media

Yeast strains used in this study are listed in Table 1. Standard rich (YPD) and synthetic complete (SC) media containing 2% glucose, 2% raffinose, or 3.5% galactose as a carbon source were used for cell growth (Rose *et al.*, 1990). A standard lithium acetate transformation method was used for the introduction of DNA into yeast (Rose *et al.*, 1990).

DNA Manipulations

Plasmids generated for this study are shown in Table 2. Site-directed mutagenesis of *DDI1* was performed by PCR with the QuickChange Site-Directed Mutagenesis Kit (Stratagene, La Jolla, CA) using plasmids bearing *HA-DDI1* or *HA-GFP-DDI1* as templates, specific oligonucleotides, and the *Pfu* Turbo DNA Polymerase (Stratagene). We constructed a variety of mutant *HA-DDI1* or *HA-GFP-DDI1* genes. For 3′ end truncations (e.g., $Ddi1^{1-75}$, $Ddi1^{1-163}$, $Ddi1^{1-326}$, $Ddi1^{1-389}$, and $Ddi1^{78-326}$), we inserted point mutations to generate premature stop codons, whereas internal deletions (e.g., $Ddi1^{\Delta 202-298}$, $Ddi1^{\Delta 323-344}$, $Ddi1^{\Delta 323-390}$, and $Ddi1^{\Delta 344-390}$) and 5′ end truncations (e.g., $Ddi1^{78-326}$ and $Ddi1^{78-428}$) were created by designing forward and reverse primers complementary to the regions flanking (downstream and upstream, respectively) the region designated for removal, such that the plasmid is synthesized and amplified with a gap. The ends of the PCR product were phosphorylated by T4 polynucleotide kinase (Fermentas, Vilnius, Lithuania) ligated to generate a closed plasmid lacking the deleted region and transformed into bacteria. The mutated genes were subjected to DNA sequencing for confirmation. Intragenomic tagging of *DDI1* with *GFP* (green fluorescent protein) was performed by homologous recombination with PCR products generated using forward and reverse oligonucleotides bearing homology to *DDI1* and the pFA6a-His3MX6-PGAL1-GFP gene-tagging plasmid as a template (Longtine *et al.*, 1998).

Table 2. Plasmids used in this study

Plasmid name	Gene expressed	Vector	Sites of cloning	Copy number	Selectable marker	Source
pAD6				2 μ	*LEU2*	J. Gerst
pAD54				2 μ	*LEU2*	J. Gerst
pADH-myc-DDI1	*myc-DDI1*	pAD6	SalI/SacI	2 μ	*LEU2*	This study
pADH-HA-GFP	*HA-GFP*	pAD54	SalI/SacI	2 μ	*LEU2*	This study
pADH-HA-DDI1	*HA-DDI1*	pAD54	SalI/SacI	2 μ	*LEU2*	This study
pADH-DDI1$^{1–75}$	*HA-DDI1$^{1–75}$*	pAD54	SalI/SacI	2 μ	*LEU2*	This study
pADH-DDI1$^{1–163}$	*HA-DDI1$^{1–163}$*	pAD54	SalI/SacI	2 μ	*LEU2*	This study
pADH-DDI1$^{1–326}$	*HA-DDI1$^{1–326}$*	pAD54	SalI/SacI	2 μ	*LEU2*	This study
pADH-DDI1$^{1–389}$	*HA-DDI1$^{1–389}$*	pAD54	SalI/SacI	2 μ	*LEU2*	This study
pADH-DDI1^{D220A}	*HA-DDI1^{D220A}*	pAD54	SalI/SacI	2 μ	*LEU2*	This study
pADH-DDI1$^{78–428}$	*HA-DDI1$^{78–428}$*	pAD54	SalI/SacI	2 μ	*LEU2*	This study
pADH-DDI1$^{Δ202–298}$	*HA-DDI1$^{Δ202–298}$*	pAD54	SalI/SacI	2 μ	*LEU2*	This study
pADH-DDI1$^{Δ323–344}$	*HA-DDI1$^{Δ323–344}$*	pAD54	SalI/SacI	2 μ	*LEU2*	This study
pADH-DDI1$^{78–326}$	*HA-DDI1$^{78–326}$*	pAD54	SalI/SacI	2 μ	*LEU2*	This study
pADH-DDI1^{C300A}	*HA-DDI1^{C300A}*	pAD54	SalI/SacI	2 μ	*LEU2*	This study
pADH-DDI1$^{Δ323–390}$	*HA-DDI1$^{Δ323–390}$*	pAD54	SalI/SacI	2 μ	*LEU2*	This study
pADH-DDI1$^{Δ344–390}$	*HA-DDI1$^{Δ344–390}$*	pAD54	SalI/SacI	2 μ	*LEU2*	This study
pADH-DDI1^{S341A}	*HA-DDI1^{S341A}*	pAD54	SalI/SacI	2 μ	*LEU2*	This study
pADH-DDI1^{T346A}	*HA-DDI1^{T346A}*	pAD54	SalI/SacI	2 μ	*LEU2*	This study
pADH-DDI1^{T348A}	*HA-DDI1^{T348A}*	pAD54	SalI/SacI	2 μ	*LEU2*	This study
pADH-DDI1-HA	*DDI1-HA*	pAD4Δ	SalI/SacI	2 μ	*LEU2*	This study
pADH-DDI1-GFP	*DDI1-HA-GFP*	pAD4Δ	SalI/SacI	2 μ	*LEU2*	This study
pADH-GFP-DDI1 $^{344–395}$	*HA-GFP-DDI1$^{344–395}$*	pAD54	SalI/SacI	2 μ	*LEU2*	This study
pADH-GFP-DDI1	*HA-GFP-DDI1*	pAD54	SalI/SacI	2 μ	*LEU2*	This study
pADH- GFP-DDI1$^{1–75}$	*HA- GFP-DDI1$^{1–75}$*	pAD54	SalI/SacI	2 μ	*LEU2*	This study
pADH-GFP-DDI1$^{1–163}$	*HA-GFP-DDI1$^{1–163}$*	pAD54	SalI/SacI	2 μ	*LEU2*	This study
pADH-GFP-DDI1$^{1–326}$	*HA-GFP-DDI1$^{1–326}$*	pAD54	SalI/SacI	2 μ	*LEU2*	This study
pADH-GFP-DDI1$^{1–389}$	*HA-GFP-DDI1$^{1–389}$*	pAD54	SalI/SacI	2 μ	*LEU2*	This study
pADH-GFP-DDI1^{D220A}	*HA-GFP-DDI1^{D220A}*	pAD54	SalI/SacI	2 μ	*LEU2*	This study
pADH-GFP-DDI1$^{78–428}$	*HA-GFP-DDI1$^{78–428}$*	pAD54	SalI/SacI	2 μ	*LEU2*	This study
pADH-GFP-DDI1$^{Δ202–298}$	*HA-GFP-DDI1$^{Δ202–298}$*	pAD54	SalI/SacI	2 μ	*LEU2*	This study
pADH-GFP-DDI1$^{Δ323–344}$	*HA-GFP-DDI1$^{Δ323–344}$*	pAD54	SalI/SacI	2 μ	*LEU2*	This study
pADH-GFP-DDI1$^{78–326}$	*HA-GFP-DDI1$^{78–326}$*	pAD54	SalI/SacI	2 μ	*LEU2*	This study
pADH-GFP-DDI1^{C300A}	*HA-GFP-DDI1^{C300A}*	pAD54	SalI/SacI	2 μ	*LEU2*	This study
pADH-GFP-DDI1$^{Δ323–390}$	*HA-GFP-DDI1$^{Δ323–390}$*	pAD54	SalI/SacI	2 μ	*LEU2*	This study
pADH-GFP-DDI1$^{Δ344–390}$	*HA-GFP-DDI1$^{Δ344–390}$*	pAD54	SalI/SacI	2 μ	*LEU2*	This study
pADH-myc-SSO1	*myc-SSO1*	pAD6	SalI/SacI	2 μ	*LEU2*	J. Gerst
YCp50-GFP-SSO1	*HA-GFP-SSO1*	YCp50	BamHI	*CEN*	*URA3*	J. Gerst

Growth Assay

Yeast cells grown to midlog phase (O.D.$_{600}$ = 0.4–0.8) were grown at 26°C, diluted serially (10-fold dilutions), and spotted onto solid YPD or selective synthetic media. Plates were incubated at different temperatures for between 36 and 48 h.

Fluorescence Microscopy

Yeast cells expressing GFP/red fluorescent protein (RFP) fusion proteins were grown to midlog phase (O.D.$_{600}$ = 0.4–0.8) at 26°C and examined by either conventional fluorescence or confocal microscopy. For induction of proteins from a *GAL1* promoter (i.e., the GGY12 strain) cells were grown either in glucose-containing or raffinose-containing media to midlog phase, washed in 10 mM Tris-EDTA buffer, pH 7.5 (TE), and incubated in galactose-containing media until GFP expression was observed (0–36 h).

Immunological Assays

Antibodies. Detection of proteins in Western blots was performed using monoclonal anti-hemagglutinin (HA; 1:1000; Roche, Indianapolis, IN), anti-GFP (1:1000; Roche), anti-myc (1:1000; 9E10, Santa Cruz Biotechnology, Santa Cruz, CA), anti-actin (1:4000; MP Biomedicals, Solon, OH) and polyclonal anti-Ddi1 (anti-Vsm1, 1:5000; Lustgarten and Gerst, 1999) antibodies. Secondary antibodies used for immunoblotting included horseradish peroxidase (HRP)-conjugated anti-mouse IgG, anti-rabbit IgG (1:10,000; Amersham Biosciences, Amersham, Buckinghamshire, United Kingdom), and HRP-conjugated anti-mouse IgG, κ light chain (1:10,000; BD Biosciences PharMingen, Franklin Lakes, NJ) used in Figures 5, A and B, and 6B.

Coimmunoprecipitation and Western Analysis. Twelve OD$_{600}$ units of midlog phase-grown yeast were used for each coimmunoprecipitation (coIP), as described previously (Gabriely *et al.*, 2007). Briefly, cells were lysed in coIP buffer (1 mM EDTA, 10 mM Tris-HCl, pH 7.5, 150 mM NaCl, 0.5% Nonidet P-40) containing protease inhibitors. For each coIP reaction, 5 μl of anti-myc antibodies was added to 500 μg of protein in a total volume of 500 μl of coIP buffer. Reactions were rotated overnight at 4°C, after which 30 μl of a protein G-agarose bead suspension (Santa Cruz Biotechnology) was added and incubated for an additional 2 h at 4°C. Five consecutive washes with coIP buffer were performed, and coIPed proteins were eluted with 30 μl of sample buffer (0.18 M Tris-HCl, pH 6.8, 4.7% SDS, 0.3% bromophenol blue, 0.42 M β-mercaptoethanol) and separated on SDS-PAGE gels. After transfer to nitrocellulose membranes, proteins were immunoblotted and detected using ECL Western blotting detection reagents (Amersham Biosciences). For coIP between myc-Sso1 and the HA-Ddi1 mutants, *ddi1*Δ cells expressing either *myc-SSO1* or one of the *HA-DDI1* mutants were grown separately and lysed, and 500 μg protein from each total cell lysate was mixed to yield 1 mg of protein in a total volume of 1 ml of coIP buffer. In this experiment, 8 μl of anti-myc antibodies were used for the coIP reaction. The rest of the IP and the detection procedures were performed as described above.

RESULTS

Construction of Ddi1 Mutants and Examination of their Expression

To better understand the roles of the different domains of Ddi1 (Figure 1A), we designed various truncation, deletion, and amino acid substitution mutants, which are schematically illustrated in Figure 1B, and tested their ability to confer function. Truncation mutants were constructed by

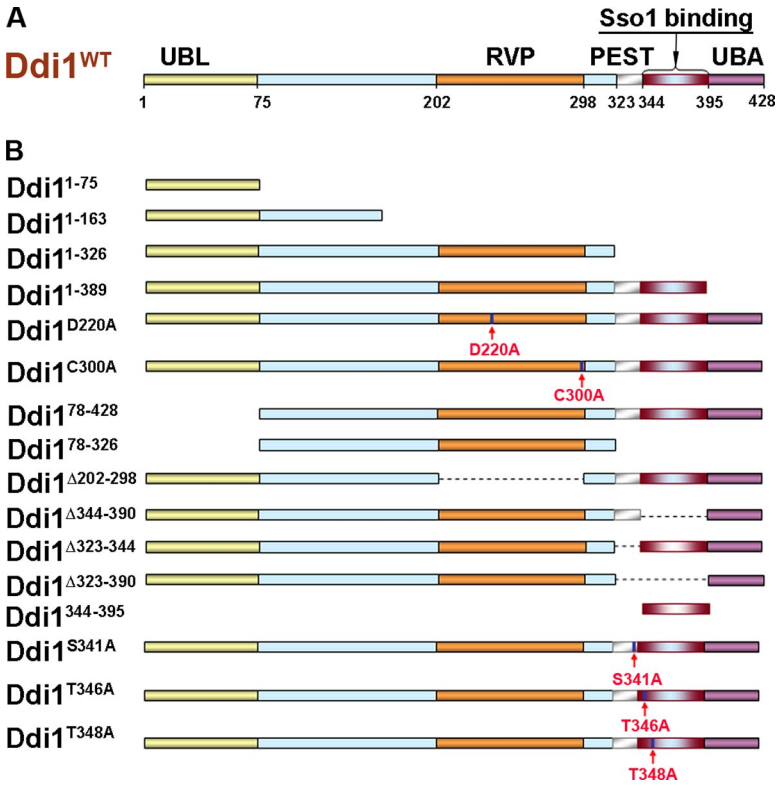

Figure 1. A schematic diagram of wild-type and mutant Ddi1 proteins. (A) Domain composition of Ddi1 in a schematic representation. Positions of the UBL, RVP, UBA, putative PEST domain, and Sso1-binding region are indicated. Numbers corresponding to the amino acid residues of the domain boundaries are shown below the protein scheme. (B) Truncation, deletion, and single amino acid substitution mutants of Ddi1. With the exception of deletion and amino acid substitution mutants, numbers at the beginning of the sequence indicate the position of the initiator methionine, whereas numbers at the end of the sequence signify the position of the last amino acid of the protein. Arrows indicate the position of amino acid substitutions. Deleted residues are indicated by the Greek delta (Δ). Note that Ddi1$^{344–395}$ was expressed as a fusion with GFP at its amino terminus.

insertion of a stop codon at different sites within the coding region of *DDI1* to yield the following: Ddi1$^{1–75}$, which consists of the UBL domain alone; Ddi1$^{1–163}$, which contains the UBL domain plus a region upstream of the RVP domain; Ddi1$^{1–326}$, which contains the UBL and RVP domains; and Ddi1$^{1–389}$, which lacks the UBA domain. In Ddi1^{D220A}, the aspartate residue necessary for potential aspartyl protease activity (D220) was substituted with alanine. In Ddi1^{C300A}, cysteine-300 (C300), which might be involved in disulfide bond formation (Sirkis *et al.*, 2006), was also substituted with alanine. Ddi1$^{78–428}$ lacks the amino-terminal UBL domain, whereas both the UBL and UBA domains were deleted in Ddi1$^{78–326}$. Ddi1$^{Δ202–298}$ lacks the entire predicted RVP domain and a putative PEST region, which was identified using the PEST-FIND algorithm (http://www.biu.icnet.uk/projects/pest/), and mapped to amino acid residues 325–343 (KSFQEGLPAPTSVTTSSDK). The PEST domain was deleted in Ddi1$^{Δ323–344}$. In general, PEST domains serve as proteolytic signals that target proteins for rapid degradation (Rechsteiner and Rogers, 1996). Ddi1$^{Δ344–390}$ lacks amino acid residues 344–390, which define the Sso1-binding region (see below), and both the PEST- and Sso1-binding regions were removed in Ddi1$^{Δ323–390}$. The defined Sso1-interacting domain of Ddi1 was fused to the carboxy terminus of GFP in GFP-Ddi1$^{344–395}$. In Ddi1^{S341A}, Ddi1^{T346A}, and Ddi1^{T348A} putative phosphorylation sites (see below) serine-341, threonine-346, and threonine-348 were substituted with alanine residues, respectively.

To examine expression of the Ddi1 mutants, each was tagged with the HA epitope at the amino terminus and expressed under the control of the constitutive *ADH1* promoter from multicopy plasmids in cells lacking *DDI1* (*ddi1*Δ cells). All HA-Ddi1 mutants were expressed and migrated at their predicted molecular masses, as determined using SDS-PAGE and Western blot analysis (Figure 2A). The smaller mutants (e.g., Ddi1$^{1–75}$ and Ddi1$^{1–163}$, which have calculated molecular masses of ~12 and ~20 kDa, respectively) were detected more clearly on higher percentage SDS-PAGE gels, as detailed in Figure 2A.

Wild-type Ddi1 runs as a doublet of 54/56 kDa on acrylamide gels (Figure 2A), and it was suggested that the band of slower mobility is a modified form of the protein (Lustgarten and Gerst, 1999). This is supported by the finding that bacterially expressed Ddi1 is not modified and runs as a single band (Lustgarten and Gerst, 1999). Although we did not know yet which modification Ddi1 undergoes, we determined the region(s) involved. By analysis of the Western blots (Figure 2A), we conclude that amino acids 344–390 are required for protein modification, because mutants that lack this region (e.g., Ddi1$^{1–75}$, Ddi1$^{1–163}$, Ddi1$^{1–326}$, Ddi1$^{78–326}$, Ddi1$^{Δ323–390}$, and Ddi1$^{Δ344–390}$) run as single bands. Interestingly, the intensity of the top band of Ddi1$^{Δ323–344}$ is reduced relative to the top band of native Ddi1, which may indicate that amino acids 323–344 (including the PEST region) are important for facilitating modification of downstream residues.

Ddi1 Homodimerization Is Mediated by the RVP Domain, But Does Not Require the Catalytic Residue, D220

It was previously found using the two-hybrid assay that Ddi1 can homodimerize, but neither the UBL nor UBA domains are involved (Bertolaet *et al.*, 2001a). Recently, it was shown by crystallography (Sirkis *et al.*, 2006) and the two-hybrid assay (Diaz-Martinez *et al.*, 2006) that the RVP-containing region undergoes homodimerization. Thus, we used the various Ddi1 mutants to determine the structural requirements for homodimerization by immunoprecipitation. We coexpressed Ddi1 mutants tagged with GFP at the amino terminus and myc-tagged full-length Ddi1 and performed coIP with anti-myc antibodies. On detection with anti-GFP antibodies we found that only Ddi1$^{1–163}$ and Ddi1$^{Δ202–298}$, which lack the RVP domain, were unable to bind full-length

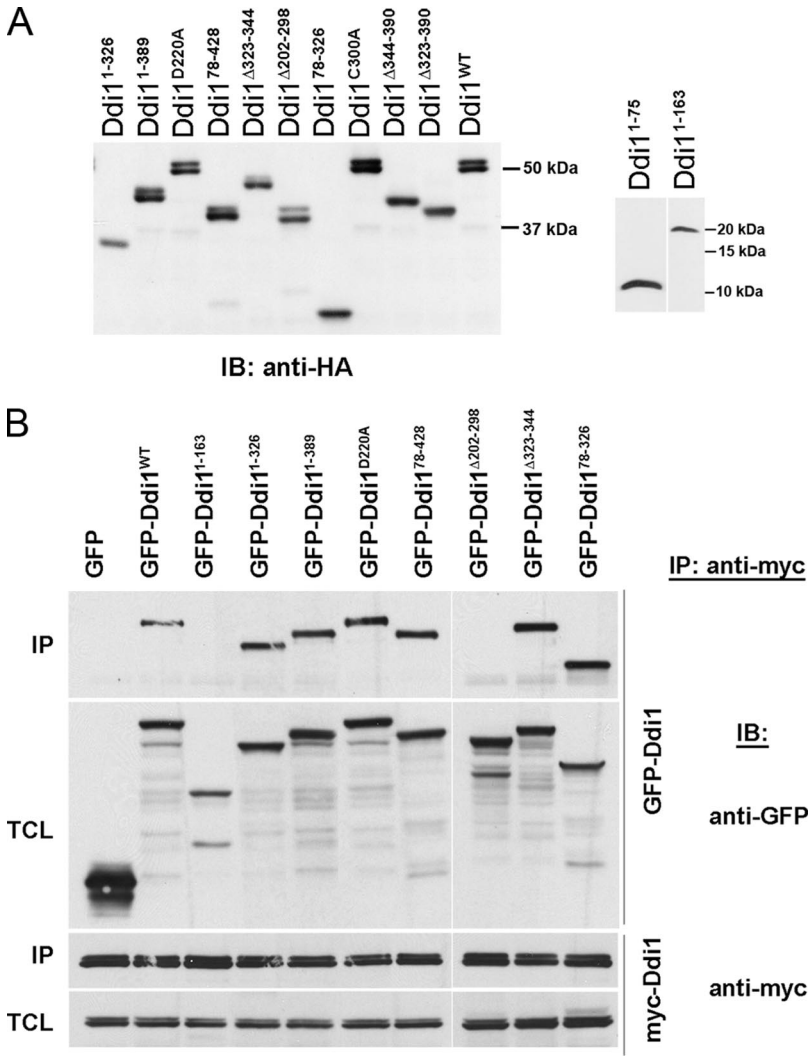

Figure 2. Expression of Ddi1 mutants and mapping the regions of protein modification and homodimerization. (A) Verification of expression of the Ddi1 mutant proteins. Yeast lacking *DDI1* (*ddi1*Δ) were transformed with multicopy plasmids overproducing wild-type HA-Ddi1 (Ddi1^{WT}, pADH-HA-DDI1) or its HA-tagged mutants (Ddi1$^{1–75}$, Ddi1$^{1–163}$, Ddi1$^{1–326}$, Ddi1$^{1–389}$, Ddi1$^{78–428}$, Ddi1$^{78–326}$, Ddi1$^{\Delta202–298}$, Ddi1$^{\Delta323–344}$, Ddi1^{D220A}, Ddi1$^{\Delta323–390}$, Ddi1$^{\Delta344–390}$, or Ddi1^{C300A}), as indicated. Yeast were grown to the midlog phase, harvested, and lysed in 1% SDS/PBS buffer containing protease inhibitors. Aliquots of 20 μg protein/lane were resolved on 10% SDS-PAGE gels, whereas aliquots of 120 or 100 μg protein/lane were taken for Ddi1$^{1–75}$ and Ddi1$^{1–163}$, respectively, and resolved on 15% gels. Ddi1 detection was performed using anti-HA (1:1000) antibodies. Size markers (in kDa) are indicated on the right side of the blots. (B) Ddi1 undergoes homodimerization via the RVP domain. *ddi1*Δ cells were cotransformed with multicopy plasmids overproducing myc-Ddi1 (pADH-myc-DDI1) and one of the GFP-tagged Ddi1 proteins: (i.e., GFP-Ddi1^{WT} or the GFP-Ddi1 mutants: GFP-Ddi1$^{1–163}$, GFP-Ddi1$^{1–326}$, GFP-Ddi1$^{1–389}$, GFP-Ddi1$^{78–428}$, GFP-Ddi1$^{78–326}$, GFP-Ddi1$^{\Delta202–298}$, GFP-Ddi1$^{\Delta323–344}$, GFP-Ddi1^{D220A} or GFP alone), as indicated above the blots. Cells were grown to the midlog phase and subjected to immunoprecipitation via anti-myc antibodies. Detection of coprecipitated proteins in immunoblots (IB) was performed by anti-GFP (1:1000) and anti-myc (1:1000) antibodies, as indicated. Samples of both the immunoprecipitation (IP) and total cell lysates (TCL; 40 μg) are presented.

Ddi1 (Figure 2B). The putative catalytic function of the RVP domain is not involved in the binding of Ddi1 monomers because a D220A substitution, which would abolish catalytic activity, did not interfere with dimerization (Figure 2B). The functionality of these GFP-tagged forms of Ddi1 and the various Ddi1 mutants was assessed in experiments listed below. Although we cannot rule out potential alterations in function because of the presence of GFP, GFP-tagged full-length Ddi1 was able to partially rescue the growth of *pds1-128* cells at restrictive temperatures (G. Gabriely and J. E. Gerst, unpublished observations). As a control, GFP expressed alone was unable to bind to full-length Ddi1 (Figure 2B).

Finally, we note that the inability of Ddi1$^{1–163}$, which contains the UBL domain, and Ddi1$^{\Delta202–298}$, which contains both the UBL and UBA domains, to bind full-length Ddi1 supports earlier observations that these domains alone are insufficient for dimerization (Kang *et al.,* 2006).

Requirements of Ddi1 for the Suppression of pds1-128 Growth Defects

Previously it was found that overexpression of *DDI1* restores the growth of a temperature-sensitive *pds1* allele, *pds 1-128*, which is defective in checkpoint control at restrictive temperatures (Clarke *et al.,* 2001). Moreover, both the UBA and RVP domains of Ddi1 (amino acids 184–285) were shown to be important for rescue (Clarke *et al.,* 2001; Diaz-Martinez *et al.,* 2006). To further characterize requirement of Ddi1 in *pds 1-128* suppression, we overproduced HA-tagged Ddi1, Ddi1$^{1–389}$, Ddi1^{D220A}, Ddi1^{C300A} (not shown), Ddi1$^{78–428}$, Ddi1$^{\Delta202–298}$, Ddi1$^{\Delta323–344}$, and Ddi1$^{78–326}$ in *pds 1-128* cells and tested their ability to restore cell growth at different semirestrictive and restrictive temperatures. According to our results (Figure 3), a lack of either the UBL or UBA domains or a deficiency in both, led to the cessation of cell growth at 35°C, much like the vector control alone. Thus, both domains are necessary for conferring growth to *pds 1-128* cells, although the lack of the UBL domain results in a slightly more severe growth defect than the deficiency of the UBA domain (Figure 3). Interestingly, either deletion of the RVP domain or an alanine substitution at D220, which disrupts the potential catalytic activity of this domain, resulted in a loss of growth rescue at the higher restrictive temperature (e.g., 37°C; Figure 3). This indicates that the RVP catalytic function may be required, in part, for suppression of the temperature sensitivity of *pds 1-128*. In contrast, another point mutation at C300 (e.g., C300A) did not affect the ability of Ddi1 to suppress *pds1-128* (our unpublished data), indicating that this residue is dispensable for rescue. As seen in Figure 2A, the mutants were expressed at similar levels,

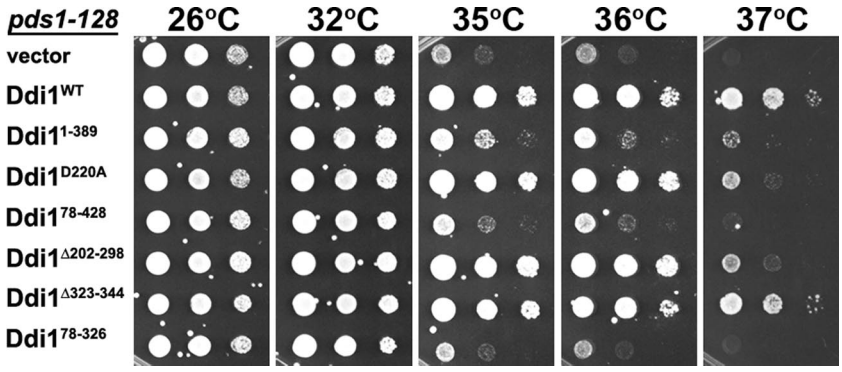

Figure 3. The UBL, UBA, and RVP domains as well as D220 of Ddi1 are required for the rescue of *pds 1-128* cells. *PDS1* mutant cells (*pds 1-128*) were transformed with vector alone (pAD54) or plasmids overproducing HA-Ddi1 (pADH-HA-DDI1; $Ddi1^{WT}$) or the various HA-Ddi1 mutants (i.e., $Ddi1^{1-389}$, $Ddi1^{D220A}$, $Ddi1^{78-428}$, $Ddi1^{\Delta 202-298}$, $Ddi1^{\Delta 323-344}$, and $Ddi1^{78-326}$). Cells grown to midlog phase at 26°C in liquid culture were diluted serially (10-fold each) and plated by drops onto solid YPD plates. Plates were incubated at different temperatures, as indicated (i.e., 26, 32, 35, 36, and 37°C) for 36–48 h, depending on the temperature.

which suggests that differences in the levels of protein cannot account for the effects seen. Our results are consistent with previous observations (Clarke *et al.*, 2001; Diaz-Martinez *et al.*, 2006), which showed that the intact protease domain is necessary for the rescue of *pds 1-128* cells at 37°C. However, because the D220A mutation does not affect homodimerization (Figure 2B), it suggests that it is the catalytic potential of this domain that rescues *pds1-128* cells and not Ddi1 dimerization, as previously suggested (Diaz-Martinez *et al.*, 2006).

GFP-Ddi1 Is Enriched in the Nucleus and Requires Both the UBL and UBA Domains for Localization

To improve on earlier studies that used immunofluorescence with anti-HA antibodies to localize HA-tagged Ddi1 (Lustgarten and Gerst, 1999), we used tagging with GFP and expressed full-length GFP-Ddi1 from a multicopy plasmid in wild-type cells (Figure 4A). Ddi1 tagged at the amino terminus with GFP showed enrichment in a large compartment that resembles the nucleus, whereas the rest of the protein was evenly spread throughout the cytoplasm (Figure 4A). The same pattern of localization was observed for full-length Ddi1 tagged with GFP at its carboxy terminus, Ddi1-GFP (Supplementary Figure S1A). The functionality of GFP-tagged Ddi1 was determined by examination of their ability to suppress the growth sensitivity of *pds1-128* cells at the restrictive temperature. Both GFP-Ddi1 and Ddi1-GFP rescued the temperature-sensitive growth of *pds 1-128* cells but less well than HA-tagged Ddi1, suggesting that GFP tagging might slightly affect the functionality of the amino-terminal UBL or carboxy-terminal UBA domains of Ddi1 (G. Gabriely and J. E. Gerst, unpublished observations). However, subcellular fractionation of cells expressing either HA- or GFP-tagged forms of Ddi1, tagged at either the amino or carboxyl terminals, demonstrated that the various forms distributed in a manner similar to native Ddi1 (Supplementary Figure S2). This rudimentary assay indicates that the different tags used do not greatly alter Ddi1 protein localization. To verify that Ddi1 is enriched in the nucleus we performed Hoechst staining of wild-type cells expressing GFP-Ddi1. Figure 4B shows the colocalization between GFP-Ddi1 labeling and Hoechst staining, which confirms nuclear accumulation of the protein. We also performed colocalization between GFP-Ddi1 and the nucleolar marker, Sik1-RFP, which labels a single dot at the nuclear periphery. As seen in Figure 4B, GFP-Ddi1 fluorescence was excluded from the nucleolar focus indicating that Ddi1 does not localize to the nucleolus.

To express GFP-Ddi1 under more native conditions, we integrated *GFP* under the control of an inducible *GAL1* promoter upstream of the *DDI1* coding region. After induction with galactose, we observed the same nuclear-cytoplasmic localization pattern with this genome-integrated form of GFP-Ddi1, as seen using multicopy expression (Figure 4A, bottom panels). To exclude the possible effect of overexpression upon GFP-Ddi1 localization, we followed its expression upon induction with galactose using both Western analysis and fluorescence microscopy. As can be seen from Supplementary Figure S1, B and C, GFP-Ddi1 expressed at 60 min was similar in amount to endogenous Ddi1 (cf. lanes 1 and 5, Supplementary Figure S1C). Moreover, GFP-Ddi1 was preferentially found in the nucleus at the same time (Supplementary Figure S1B), which indicates that Ddi1 is directed to this compartment at the early stages of its expression. Furthermore, GFP-Ddi1 expressed from the genome fractionated in a similar manner to both native and plasmid-expressed Ddi1 (Supplementary Figure S2). Although a large-scale protein localization study, employing GFP-tagging at the carboxy terminus of the proteins, demonstrated a cytoplasmic pattern of localization for Ddi1 (Huh *et al.*, 2003), we observed nuclear enrichment using all forms of expression, including multicopy expression of either amino- or carboxy-terminal GFP-tagged Ddi1 (Figure 4A and Supplementary Figure S1A), single-copy expression of Ddi1 tagged at the amino terminus with GFP (our unpublished data), and genomic tagging of the amino-terminal of Ddi1 (Figure 4A, Supplementary Figure S1, B and C). This data suggests that Ddi1 can reside within the nucleus.

To identify the domain(s) required for the accumulation of GFP-Ddi1 in the nucleus we expressed the Ddi1 mutants tagged at their amino terminus with GFP in cells lacking *DDI1*. This allows us to exclude the possibility of GFP-tagged Ddi1 or the GFP-tagged Ddi1 mutants sequestering to the nuclear compartment through binding to endogenous Ddi1 (Figure 2B). Although all GFP-Ddi1 mutants could be localized to the nucleus (as was GFP alone), specific nuclear enrichment was observed only for the full-length GFP-Ddi1 and mutants that contain both the UBL and UBA domains (e.g., $Ddi1^{D220A}$, $Ddi1^{C300A}$, $Ddi1^{\Delta 202-298}$, $Ddi1^{\Delta 344-390}$, $Ddi1^{\Delta 323-390}$, and $Ddi1^{\Delta 323-344}$; Figure 4C). Thus, nuclear enrichment requires both the UBL and UBA domains of GFP-Ddi1. The minor accumulation of some UBL- or UBA-deficient GFP-Ddi1 mutants in the nucleus could be explained by sequestration via nuclear Rad23 (Huh *et al.*, 2003), which heterodimerizes with Ddi1 through either the UBL or UBA domains (Bertolaet *et al.*, 2001a; Kang *et al.*, 2006). Interestingly, GFP-$Ddi1^{C300A}$ tends to accumulate at one (Figure 4C) or more punctuate structures inside the cell, although the site of localization has not been identified yet.

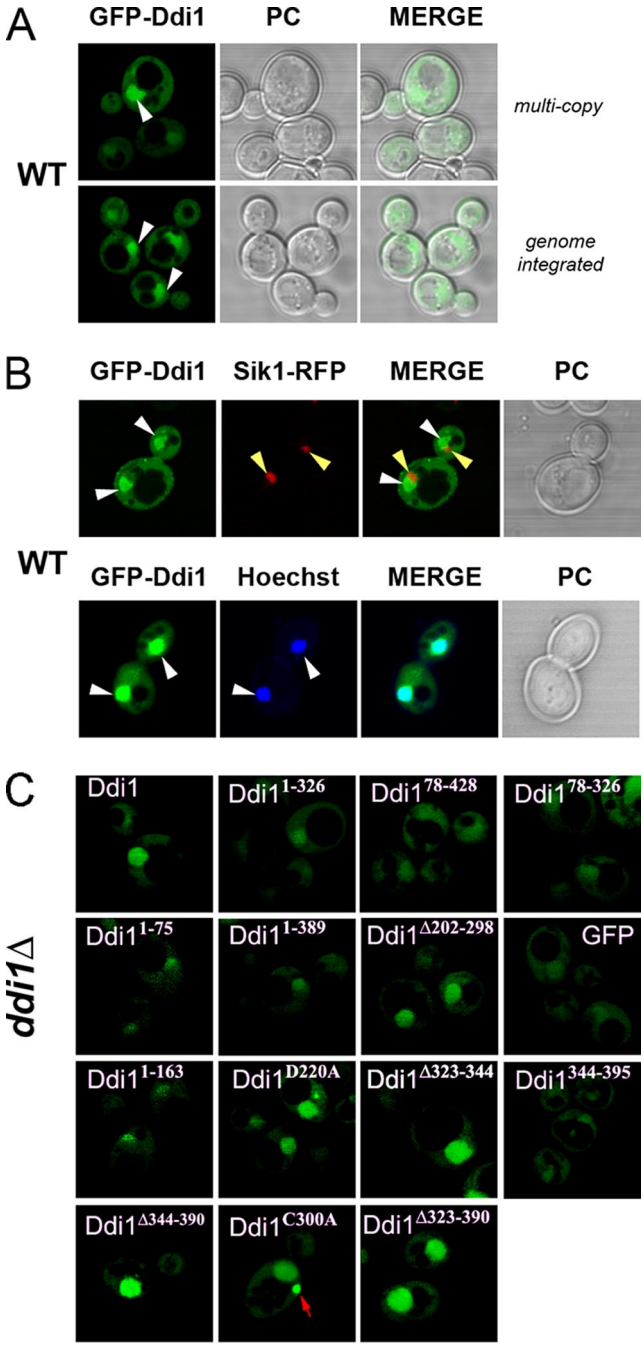

Figure 4. Nucleo-cytoplasmic localization of GFP-Ddi1 in wild-type cells. (A) *GFP-DDI1* expressed from a multicopy plasmid or from the genome gives nucleo-cytoplasmic labeling. Wild-type cells (W303; WT) expressing *GFP-DDI1* from either a multicopy plasmid (pADH-GFP-DDI1; top panel) or from the genome (genome integrated GGY12 cells; bottom panel) were examined. Genomic *GFP-DDI1* expression was induced by growth in galactose-containing media for 16–20 h. Cells grown to midlog phase were taken for analysis by confocal fluorescence microscopy. Both phase contrast (PC) and merged (MERGE) light and fluorescence panels are shown. Arrows indicate accumulation of GFP-Ddi1 in large epivacuolar compartments. (B) Colocalization of GFP-Ddi1 with nuclear markers. Wild-type cells (ATCC[a] 201389) bearing an integrated copy of nucleolar marker *SIK1-RFP* were transformed with a multicopy plasmid overproducing GFP-Ddi1 (pADH-GFP-DDI1) and examined by confocal microscopy (top panel). Hoechst staining was performed on wild-type cells (WT, BY4741) expressing *GFP-DDI1* from multicopy plasmid, which were grown to midlog phase and incubated with Hoechst 33342 (0.2 mg/ml final concentration; Molecular Probes, Eugene, OR) for 5 min followed by two washes in 10 mM Tris-EDTA buffer, pH 7.5. White arrows indicate the position of nuclei, and yellow arrows indicate nucleoli. (C) The UBL and UBA domains of Ddi1 are required for its nuclear enrichment. Yeast bearing a disruption in *DDI1* (*ddi1*Δ) were transformed with multicopy plasmids producing GFP, GFP-Ddi1 (Ddi1), or the GFP-Ddi1 truncation (Ddi1$^{1-75}$, Ddi1$^{1-163}$, Ddi1$^{1-326}$, Ddi1$^{1-389}$, Ddi1$^{78-428}$, Ddi1$^{78-326}$, Ddi1$^{\Delta 202-298}$, Ddi1$^{\Delta 323-344}$, Ddi1$^{\Delta 344-390}$, Ddi1$^{344-395}$, and Ddi1$^{\Delta 323-390}$) and single amino acid substitution mutants (Ddi1^{C300A} and Ddi1^{D220A}). An arrow points out the accumulation of GFP-Ddi1^{C300A} in the cytoplasm in cells producing GFP-Ddi1^{C300A}.

Identification of the Sso1-binding Domain in Ddi1

We previously found that Ddi1 interacts physically with the exocytic t-SNARE, Sso1, both in vitro and in vivo, and in a manner independent of the UBA domain of Ddi1 (Marash and Gerst, 2003). To determine which region of Ddi1 is responsible for binding to Sso1, we performed coIP between overexpressed myc-tagged Sso1 and the Ddi1 mutants tagged at the amino terminus with HA epitope, using anti-myc antibodies. As shown in Figure 5A, only the Ddi1 mutants lacking the carboxy-terminal-most 100 amino acids (i.e., Ddi1$^{1-326}$ and Ddi1$^{78-326}$) were unable to coimmunoprecipitate with myc-Sso1, indicating that these residues might be involved in Ddi1 binding to Sso1. Because the UBA domain (residues 395–428) is not required for Sso1 binding (Marash and Gerst, 2003 and Figure 5A), we cloned the DNA sequence corresponding to residues 344–395 downstream of the sequence encoding a GFP-HA fusion and expressed this in wild-type cells along with myc-Sso1. *GFP-HA-DDI1$^{344-395}$* expression produced a fusion protein at levels similar to the full-length HA-Ddi1 (Figure 5B). Moreover, GFP-HA-Ddi1$^{344-395}$ coprecipitated with myc-Sso1, indicating that the 52 amino acid residues of region 344–395 is sufficient for Sso1 binding. We note that less Sso1 binding to this mutant was observed, in comparison to full-length GFP-HA-Ddi1, perhaps because the structure of the interacting domain is not well-maintained in the mutant protein.

In parallel, we performed reciprocal coIP experiments to precipitate endogenous Sso1/2 through overexpressed HA-Ddi1 or myc-Ddi1, using anti-HA or anti-myc antibodies, respectively. However, we were unable to detect the native paralogs using anti-Sso antibodies (G. Gabriely and J. E. Gerst, unpublished observations). This may indicate that native Sso is not available in sufficient amounts to allow for the detectable association with overexpressed, tagged Ddi1 or that antibody binding interferes with the Ddi1-Sso1 interaction.

We next examined whether the Sso1-Ddi1 interaction occurs at the plasma membrane, where Sso1 is localized, or at different stages of endocytic transport. To do this, we expressed myc-Sso1 in endosomal protein sorting mutants defective in 1) internalization from the plasma membrane, (i.e., *end4-1*); 2) late endosomal transport (i.e., a class D *vps* mutant, *pep12*Δ); and 3) MVB-mediated protein sorting (a class E *vps* mutant, *vps4*Δ). We found that endogenous Ddi1 is produced at similar levels in the different mutants as in wild-type cells, although the level of myc-Sso1 was considerably less in *pep12*Δ cells for yet unknown reasons. We precipitated myc-Sso1 from the different strains and followed coIP of endogenous Ddi1 using anti-Ddi1 antibodies. As can be seen (Supplementary Figure S3A), Ddi1 was coprecipitated at similar amounts from wild-type, *end4-1*, and *vps4*Δ cells. Less Ddi1 was coprecipitated from *pep12*Δ cells

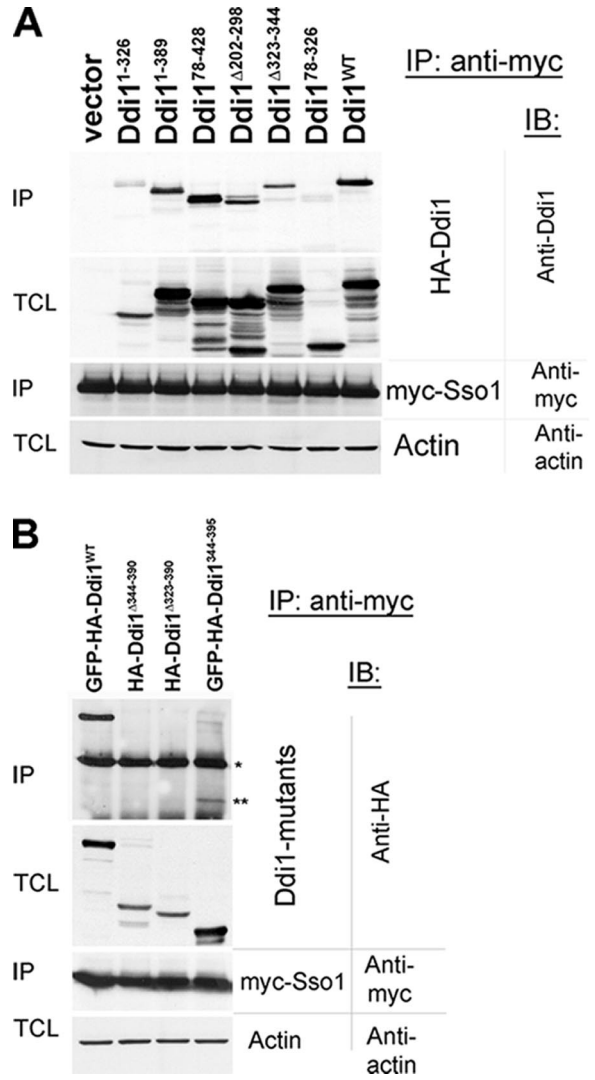

Figure 5. Identification of the Sso1-binding region. (A and B) A region comprising amino acid residues 344–395 mediates the interaction of Ddi1 with Sso1. Total cell lysates derived from *DDI1* deficient cells (*ddi1*Δ) overproducing myc-Sso1 (pADH-myc-Sso1) were mixed with lysates derived from *ddi1*Δ cells expressing wild-type or mutant HA-tagged Ddi1 proteins. (A) Lysates from *ddi1*Δ cells producing myc-SSO1 were mixed either with *ddi1*Δ cell lysates producing wild-type HA-Ddi1 (Ddi1^{WT}; plasmid pADH-HA-DDI1) or one of the Ddi1 mutants (e.g., HA-Ddi1$^{1–326}$, HA-Ddi1$^{1–389}$, HA-Ddi1$^{78–428}$, HA-Ddi1$^{\Delta202–298}$, HA-Ddi1$^{\Delta323–344}$, HA-Ddi1$^{78–326}$). (B) Lysates from *ddi1*Δ cells producing myc-Sso1 were mixed with *ddi1*Δ cell lysates producing wild-type GFP-HA-Ddi1 (GFP-HA-Ddi1^{WT}; plasmid pADH-GFP-DDI1) or one of the Ddi1 mutants (e.g., HA-Ddi1$^{\Delta323–390}$, HA-Ddi1$^{\Delta344–390}$, and GFP-HA-Ddi1$^{344–395}$). Coimmunoprecipitation (IP) was performed using anti-myc antibodies. Vector indicates cells transformed with an empty plasmid. The detection of precipitated proteins in immunoblots (IB) was performed using anti-Ddi1 (anti-Vsm1, 1:5000), anti-myc (1:1000), anti-HA (1:1000), or anti-actin (1:5000) antibodies. Samples of the total cell lysates (TCL) are shown (40 μg protein per lane). The single asterisk (*) in B indicates the position of heavy chain of the anti-myc antibody used in the coIP. The two asterisks (**) indicate the position of GFP-HA-Ddi1$^{344–395}$. Actin was detected in the TCLs as a control for gel loading.

probably because of the lower levels of myc-Sso1 expression in these cells. We therefore conclude that no difference in the interaction between myc-Sso1 and Ddi1 is observed upon disruption of the different stages of endosomal sorting. This indicates that the Sso1-Ddi1 interaction probably occurs at the plasma membrane, which is not affected in these transport mutants. As Ddi1 may localize to different cellular compartments, including the plasma membrane (Lustgarten and Gerst, 1999), it is likely to interact with Sso1 there. Although the deletion of *DDI1* does not alter the stability of Sso1 (Marash and Gerst, 2003), we examined whether it alters the localization of GFP-Sso1. We found that GFP-Sso1 localizes mainly to the plasma membrane and to small cytoplasmic structures (likely to be Golgi-early endosomes) in wild-type cells (Valdez-Taubas and Pelham, 2003 and Supplementary Figure S3B). This pattern of localization was maintained in *ddi1*Δ cells, however, GFP-Sso1 accumulated at what appear to be enlarged late endosomes in the class E *vps4*Δ mutant (Supplementary Figure S3B). Because GFP-Ddi1 also associates with these structures in class E mutants (G. Gabriely and J. E. Gerst, unpublished observations), Ddi1-Sso protein complexes may not be restricted to the plasma membrane. In an earlier work (Lustgarten and Gerst, 1999), we showed that Ddi1 interacts with the Snc1 and Snc2 v-SNAREs. Unfortunately, reciprocal coIP experiments to repeat these interactions using either endogenous or overexpressed Snc proteins were largely unsuccessful (G. Gabriely and J. E. Gerst, unpublished observations). It may be that Sso t-SNAREs bound to the Snc v-SNAREs in the SNARE complex were somehow able to coprecipitate Ddi1 in these earlier assays. In conclusion, Ddi1 interacts with the Sso1 t-SNARE via a specific region of 52 amino acids that is located between the RVP and UBA domains.

Ddi1 Is Modified by Phosphorylation on Threonines Located in the Sso1-binding Domain and T348 Is Necessary for Ddi1-Sso1 Interactions

To identify the nature of the posttranslational modification of Ddi1 we used mass spectrometry (MS). We chose to analyze the Ddi1$^{\Delta202–298}$ mutant lacking the RVP domain because it undergoes modification (see lane 6, Figure 2A), and both modified and nonmodified forms are better resolved on SDS-PAGE gels. HA-Ddi1$^{\Delta202–298}$ was first immunoprecipitated from lysates derived from yeast overproducing the protein and resolved by SDS-PAGE. Both bands of the Ddi1 doublet were identified by protein staining, cut separately from the gel, digested with trypsin, and analyzed by liquid chromatography–tandem MS (LC-MS/MS). Peptide coverage for both bands was essentially 100%. Multiple monophosphorylated peptides, which covered amino acids 326–351 of Ddi1 (KSFQEGLPAPTSVTTSSDKPLTPTKT), were identified exclusively from the upper band of the doublet using LC-MS/MS, due to the increase in mass. This increase corresponded to ~80 Da and analysis with Sequest software predicted several potential phosphorylation sites mapping to serine-341 (S341), threonine-346 (T346), or -348 (T348).

To determine the actual contribution of these amino acids to doublet formation (Figure 2A), each was substituted with alanine, and the resulting mutants resolved using Western analysis. As can be seen in Figure 6A, T346 appears to be the main site for modification because a point mutation (T346A) abolished doublet formation. Substitution of T348 with alanine led to a partial reduction of the top band, indicating that this threonine is either modified sometimes or is involved in the modification of T346. In contrast, S341 does not seem essential for the modification, because an alanine substitution at this residue did not change the doublet formation. According to these results, we predict that Ddi1 under-

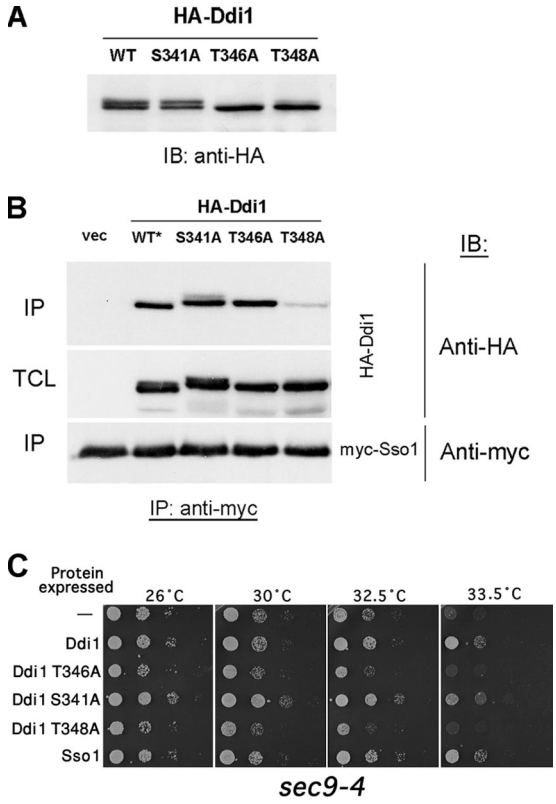

Figure 6. Ddi1 is modified at specific threonines and T348 plays an important role in Sso interaction and function. (A) Substitution of T346 and T348 abolishes Ddi1 modification. *DDI1* deletion mutant cells (*ddi1*Δ) were transformed with plasmids expressing wild-type *HA-DDI1* (WT; pADH-HA-DDI1) and mutants *HA-DDI1*^{S341A} (S341A), *HA-DDI1*^{T346A} (T346A), and *HA-DDI1*^{T348A} (T348A). Cells were grown to midlog phase and lysed, and 30 μg/lane protein was separated by SDS-PAGE. Protein expression was detected using anti-HA antibodies (1:1000). (B) Threonine-348 is important for Ddi1 binding to Sso1. CoIP was performed as described in Figure 5, A and B. Lysates from *ddi1*Δ cells producing myc-Sso1 were mixed either with *ddi1*Δ cell lysates producing wild-type Ddi1-HA (WT*, plasmid pADH-HA-DDI1) or one of the HA-Ddi1 mutants (HA-Ddi1^{S341A}, HA-Ddi1^{T346A}, or HA-Ddi1^{T348A}; plasmids pADH-HA-Ddi1^{S341A}, pADH-HA-Ddi1^{T346A}, or pADH-HA-Ddi1^{T348A}, accordingly). An asterisk indicates that the wild-type Ddi1 used here was tagged with a shorter HA tag at the carboxy-terminus than the Ddi1 mutants, which were tagged at the amino-terminus with a somewhat larger HA tag. Note, that the short HA tag results in faster mobility on SDS-PAGE gels. (C) Phosphorylatable Ddi1 rescues the growth of *sec9-4* cells. *sec9-4* cells transformed with plasmids that overproduce native HA-Ddi1 (Ddi1), HA-Ddi1^{S341A} (Ddi1 S341A), HA-Ddi1^{T346A} (Ddi1 T346A), HA-Ddi1^{T348A} (Ddi1 T348A), or myc-Sso1 protein (Sso1) or transformed with vector alone (−) were grown to midlog phase, diluted serially (10-fold), and plated onto solid synthetic selective medium preincubated at the given temperatures. Cells were grown for 48 h.

goes phosphorylation on T346 and, possibly, T348 in the Sso1-binding region.

As shown above, the putative phosphorylation sites (e.g., T346 and T348) are located at the Sso1-binding region of Ddi1 and, therefore, might be involved in the interaction between these proteins. To examine this possibility, we performed coIP by precipitating myc-Sso1 with anti-myc antibodies and detecting for the presence of coprecipitated HA-tagged Ddi1 mutants (Ddi1^{S341A}, Ddi1^{T346A}, and Ddi1^{T348A}). Surprisingly, the alteration of T348 significantly abrogated myc-Sso1 binding to Ddi1, whereas point mutations in S341 and T346 had no effect on this interaction (Figure 6B).

Finally, we examined whether the alanine substitutions had effects upon Sso t-SNARE function in vivo. We overproduced Ddi1, Ddi1^{S341A}, Ddi1^{T346A}, Ddi1^{T348A}, and Sso1 in a temperature-sensitive *sec9-4* t-SNARE mutant strain using multicopy plasmids and examined cell growth at various temperatures (Figure 6C). Native Ddi1 was seen to enhance the growth of *sec9-4* cells at elevated temperatures (i.e., >26°C; Figure 6C), which differs somewhat from our original finding that *DDI1/VSM1* overexpression suppresses the growth of these cells (Lustgarten and Gerst, 1999). However, the version of *DDI1* used in this study (for all constructs) is a corrected version of the original clone (Lustgarten and Gerst, 1999), which was found to have two point mutations that were likely created during PCR amplification. These mutations resulted in amino acid substitutions R309G and Q428E, the former being in the Sso-binding domain. Correction of these mutations leads to an opposite effect (i.e., rescue of *sec9-4* cells), indicating that one or both of the mutations interfere with the Ddi1-Sso interaction to some degree. Interestingly, the Ddi1^{S341A} alanine substitution mutant was found to rescue the growth of *sec9-4* cells at semirestrictive temperatures better than native Ddi1 (Figure 6C). In contrast, overproduction of the Ddi1^{T346A} and Ddi1^{T348A} alanine substitution mutants, which are either underphosphorylated or nonphosphorylated (Figure 6A), were unable to ameliorate the growth of these cells. Thus, a loss in phosphorylation abrogates any beneficial effect that Ddi1 overproduction might confer to this temperature-sensitive t-SNARE. We note that *SSO1* overexpression also rescued the *sec9-4* mutant (Figure 6C), indicating that elevated Sso1 levels alone enhance the function of the mutant Sec9 t-SNARE. Thus, overproduction of a form of Ddi1 able to undergo phosphorylation (e.g., native Ddi1 or Ddi1^{S341A}) conferred rescue in a manner identical to Sso1 overproduction. Therefore, phosphorylation appears to enhance the functional consequences of the Ddi1-Sso1 interaction.

DISCUSSION

In this study we used truncation, deletion, and amino acid substitution mutants of Ddi1/Vsm1 to map its known cellular functions to distinct regions/domains of the protein. These data are summarized in Table 3 and presented schematically in Figure 7. In principle we have more accurately mapped the regions for Ddi1 homodimerization and suppression of *pds 1-128* cell cycle mutant, as well as demonstrating the requirements for nuclear localization, Sso1 t-SNARE binding, and posttranslational modification by phosphorylation for the first time. We found that the RVP domain, but not the catalytic aspartate residue D220, is required for homodimerization (Figure 2B). In contrast, D220 is needed for suppression of temperature sensitivity of *pds 1-128* cells along with the UBL and UBA domains (Figure 3). The latter domains are also necessary for the nuclear enrichment of Ddi1, which we show for the first time (Figure 4). Finally, we demonstrate that a region separating the RVP and UBA domains is sufficient for binding to the Sso1 t-SNARE (Figure 5), thus defining a new domain for this ubiquitin receptor. This same region appears to undergo modification (Figure 2A), which was identified by MS as phosphorylation. A functional role for the modification of threonine-348 was demonstrated for Sso1 binding.

Table 3. A summary of the results obtained for Ddi1 and the Ddi1 mutants

Name	Modification (doublet)	Ddi1 homodimerization	Sso1-binding	*pds1-128* suppression	Nuclear enrichment
Ddi1	Yes	+++	+++	+++	+++
$Ddi1^{1–75}$	No	NT[a]	NT	NT	+
$Ddi1^{1–163}$	No	−	−	NT	+
$Ddi1^{1–326}$	No	+++	+++	NT	+
$Ddi1^{1–389}$	Yes	+++	+++	+	+
$Ddi1^{D220A}$	Yes	+++	NT	+++	+++
$Ddi1^{78–428}$	Yes	+++	+++	+/−	+
$Ddi1^{\Delta 202–298}$	Yes	−	+++	++	+++
$Ddi1^{\Delta 323–344}$	Partial	+++	+++	+++	+++[b]
$Ddi1^{78–326}$	No	+++	−	−	+
$Ddi1^{\Delta 323–390}$	No	NT	−	NT	+++
$Ddi1^{\Delta 344–390}$	No	NT	−	NT	+++[b]
$Ddi1^{C300A}$	Yes	NT	+++	NT	+++[c]
$Ddi1^{344–395}$	No	NT	+	NT	+
$Ddi1^{S341A}$	Yes	NT	+++	NT	NT
$Ddi1^{T346A}$	No	NT	+++	NT	NT
$Ddi1^{T348A}$	Partial	NT	+/−	NT	NT
Vector control	NT	−	−	−	NT
GFP control	NT	NT	NT	NT	+
Ddi1 region responsible:	Amino acids 344–390, T346 and T348	RVP	Amino acids 344–395, T348	UBL and UBA (RVP and D220)	UBL and UBA

[a] NT, not tested.

[b] Intranuclear accumulation of GFP-Ddi1.

[c] Intranuclear and cytoplasmic accumulation of GFP-Ddi1.

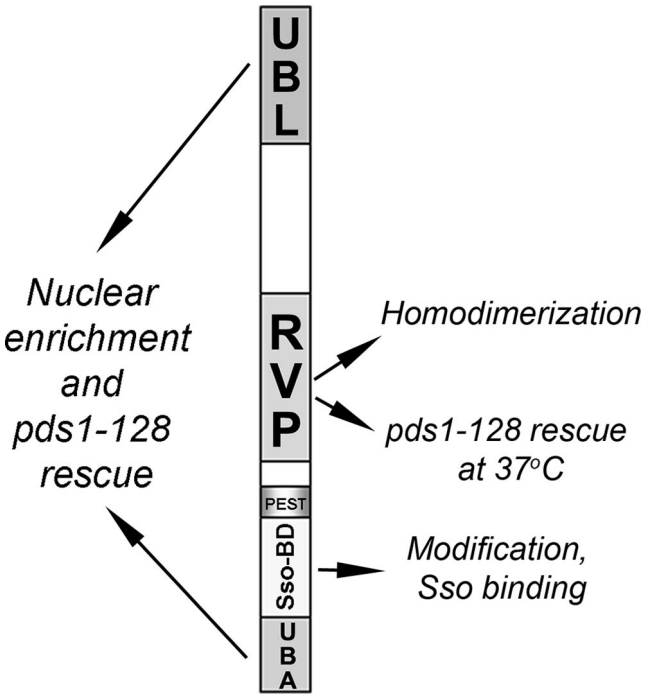

Figure 7. A schematic representation of the different domains of Ddi1 and their involvement in cellular processes in yeast. The Ddi1 protein is composed of the UBL, UBA, RVP, Sso-binding domain (Sso-BD), and PEST region. The RVP domain of Ddi1 mediates homodimerization as well as rescue of the *pds1-128* mutant at 37°C. Both the UBL and UBA domains are involved in the nuclear enrichment of Ddi1 and the suppression of *pds1-128* cells, suggesting that they are related processes. The phosphorylation of Ddi1 occurs on residues T346 and T348, and T348 mediates the interaction with Sso1.

Homodimerization of Ddi1

Like other UBL-UBA family members in *S. cerevisiae*, namely Dsk2 (Sasaki *et al.*, 2005) and Rad23 (Bertolaet *et al.*, 2001a; Kang *et al.*, 2006), Ddi1 is able to homodimerize (Bertolaet *et al.*, 2001a). However, in contrast to its paralogs Ddi1 homodimerization requires the RVP domain (Figure 2B and Diaz-Martinez *et al.*, 2006). This result is consistent with previous observations showing either dispensability of the UBL and UBA domains (Bertolaet *et al.*, 2001a; Kang *et al.*, 2006) or necessity for residues 184–285 in Ddi1 homodimerization (Diaz-Martinez *et al.*, 2006). It is noteworthy that the aspartyl protease domains are well conserved throughout evolution and were shown to be active when present in their dimeric form (Miller *et al.*, 1989). Recently, the crystal structure of the RVP domain of Ddi1 was resolved in its dimeric form and was shown to have strong structural similarity to other retroviral proteases (Sirkis *et al.*, 2006). This suggests that Ddi1 may have proteolytic activity, although bona fide substrates have yet to be found. However, the catalytic aspartate is not necessary for homodimerization to occur (Figure 2B), which suggests that the ability to homodimerize is independent of potential catalytic function. We did not examine the ability of $Ddi1^{C300A}$ to homodimerize, but a recent study reported that C300 is not involved in this process (Diaz-Martinez *et al.*, 2006). Interestingly, the results presented in Figure 2B indicate that an intramolecular UBL-UBA interaction in Ddi1 probably does not occur, which supports an earlier model (Kang *et al.*, 2006). In conclusion, the RVP domain of Ddi1 mediates homodimerization in vivo, like in other conserved aspartyl proteases, suggesting a possible involvement in proteolysis (Krylov and Koonin, 2001).

Suppression of the pds1-128 Mutant

Our results confirm requirement of the UBA (Clarke *et al.*, 2001) and RVP (Diaz-Martinez *et al.*, 2006) domains of Ddi1

in rescue of the temperature-sensitive growth of *pds1-128* cells and further show that the UBL domain is also involved (Figure 3). In contrast, the UBL domain of Rad23 is dispensable for the suppression of growth defects in *pds1-128* cells (Clarke *et al.,* 2001), indicating that the UBL domain of Ddi1 functions differently from that of Rad23. Both Rad23 and Ddi1 play positive roles in restoring the growth of cells bearing a mutation in Pds1, which is a regulator of sister chromatid separation in mitosis and a substrate of the proteasome (Clarke *et al.,* 2001). It was suggested that the UBA domain of Rad23 (and probably that of Ddi1) binds directly to ubiquitin modifications on Pds1 to protect the protein from degradation (Clarke *et al.,* 2001). By demonstrating the requirement of the UBL domain of Ddi1 in suppression of the *pds1-128* mutant (Figure 3), we prove that the proteasome-interacting domain is no less important than the UBA domain. Together, both the UBL and UBA domains are required for the suppression of growth defects in *pds 1-128* cells.

It is known that the UBL and UBA domains of ubiquitin receptors are involved in protein targeting to the proteasome for degradation (Saeki *et al.,* 2002; Elsasser *et al.,* 2004; Kim *et al.,* 2004). In particular, the UBL domain of Ddi1 anchors to the proteasome via the Rpn1 subunit (Kaplun *et al.,* 2005). Thus, Ddi1 is probably not involved in the direct stabilization of Pds1-128, but may act as an ubiquitin receptor involved in the degradation of a putative Pds1 regulator via the proteasome. A similar role for Ddi1 was shown previously for another substrate, HO endonuclease (Kaplun *et al.,* 2005). Alternatively, because both the UBL and UBA domains are required for Ddi1 to undergo nuclear enrichment, we speculate that the failure of mutants lacking these domains to become nuclear-enriched may result in their inability to rescue *pds1-128* growth defects. It was previously reported (Diaz-Martinez *et al.,* 2006), and we observed here (Figure 3), that the RVP domain is also important for the rescue of *pds1-128* cells at 37°C. However, loss of the RVP domain only partially affects the ability of Ddi1 to suppress the *pds1-128* defect (Figure 3). Moreover, in contrast to the suggestion that Ddi1 homodimerization is required for rescue (Diaz-Martinez *et al.,* 2006), we show that the putative aspartyl protease activity, dependent on D220, is actually involved (Figure 3). This suggests that a potential proteolytic substrate of Ddi1 may be involved in regulating Pds1 activity.

Nuclear Enrichment of Ddi1

By employing GFP-tagging we showed that amino- or carboxy-terminal fusions (GFP-Ddi1 or Ddi1-GFP, respectively; Figure 4, Supplementary Figure S1, and our unpublished observations) localize predominantly to the nucleus in wild-type cells. This observation is consistent with other data suggesting a role for Ddi1 in the nucleus. First, Pds1 functions in the nucleus during mitosis and, thus, rescue of its mutant allele by *DDI1* overexpression is consistent with a nuclear role for Ddi1 (Quimby *et al.,* 2005). Second, HO endonuclease is a Ddi1 target substrate that undergoes rapid degradation in the nucleus (Kaplun *et al.,* 2005). Third, Ddi1 may be enriched in the nucleus due to its association with proteasomes (Kaplun *et al.,* 2005), which concentrate in the nucleus in yeast (Wilkinson *et al.,* 1998; Russell *et al.,* 1999). Finally, the ability of Ddi1 to enter the nucleus may explain interactions observed between Ddi1 and Bub2, another checkpoint factor, in a large-scale two-hybrid screen (Bardin and Amon, 2001). Notably, other yeast UBL-UBA paralogs, Rad23 and Dsk2, also localize preferentially to the nucleus (Biggins *et al.,* 1996; Huh *et al.,* 2003), which could imply a common function (together with Ddi1) in nuclear-associated ubiquitin-dependent proteolysis. As both the UBL and UBA domains are also important for the nuclear enrichment of GFP-Ddi1 (Figure 4C), it suggests that the localization of Rad23 and Dsk2 to the nucleus is dependent on these domains as well (Figure 4). In an earlier study, we suggested that Ddi1 can partially associate with the plasma membrane (Lustgarten and Gerst, 1999), which would explain its ability to interact with exocytic v- and t-SNAREs (Lustgarten and Gerst, 1999; Marash and Gerst, 2003). Either the techniques used then were of insufficient resolution to show the nuclear localization of Ddi1 or, perhaps, GFP-tagged Ddi1 preferentially localizes to the nucleus and not the plasma membrane. Alternatively, the two point mutations discovered in the original *DDI1* clone may have influenced protein localization to some degree. In any event, this work shows that Ddi1 is found in the nucleus, which would go far to explain its role in interacting with cell cycle–related proteins and mediating their stability.

Sso1 t-SNARE Interaction

Ddi1 was independently isolated and characterized by us as a potential SNARE regulator involved in negative regulation of the late secretory pathway via its ability to bind to exocytic v- and t-SNAREs (e.g., Snc1/2 and Sso1, respectively; Lustgarten and Gerst, 1999; Marash and Gerst, 2003). In the case of the t-SNARE binding, phosphorylation of the autoinhibitory domain of Sso1 increased its affinity for Ddi1 both in vivo and in vitro (Marash and Gerst, 2003). In addition, we found that Ddi1 binds Sso1 with no requirement for the UBA domain (Marash and Gerst, 2003). Here, we mapped the t-SNARE interaction domain to amino acids 344–395 in Ddi1 (Figure 5). This region of the protein does not coincide with any known domain function of Ddi1 and thus constitutes a novel protein-interacting region located between the RVP and UBA domains. Importantly, this finding indicates that the function of Ddi1 as an ubiquitin receptor requiring the UBL and UBA domains is probably independent of its interactions with the exocytic machinery. Likewise, as the RVP domain is not required for the Sso1-Ddi1 interaction, it suggests that the putative proteolytic activity of Ddi1 is also not involved either. It is noteworthy that the Sso-interaction region in Ddi1 undergoes modification (Figure 2A) at specific threonines (T346 and T348; Figure 6A). Interestingly, $Ddi1^{T348A}$ (which undergoes partial modification at T346) does not bind Sso1, whereas $Ddi1^{T346A}$, which is not modified, interacts normally with Sso1. This observation suggests that the modification of T348 plays a role in the regulation of Ddi1 binding to Sso1.

Modification of Ddi1

It was previously suggested that Ddi1 undergoes posttranslational modification because it runs as a doublet in Western blots of yeast cell lysates, but not bacterial cell lysates (Lustgarten and Gerst, 1999). Here we mapped the putative region of modification to amino acids 344–390 (Figure 2A), which are also involved in Sso1 binding (Figure 5, A and B). We note that the region between the RVP and UBA domains contains a PEST motif and is a region of low complexity rich in proline, serine, threonine, and glycine residues that is predicted to be poor in secondary structure (Sirkis *et al.,* 2006). Moreover, the presence of multiple serines and threonines in this area suggested to us that Ddi1 is likely to be modified by phosphorylation. Indeed, through MS analysis monophosphorylated peptides were identified and indicated several potential residues for modification (e.g., S341, T346, and T348). By using site-directed mutagenesis we identified T346 as the main modified residue, whereas

T348 seems to be partially involved in this modification. Interestingly, T348 but not T346 is required for the physical interaction with Sso1, which shows the importance of specific Ddi1 modification sites in Sso. Amino acid residues 323–344 may facilitate modification because the high (molecular mass) band of the Ddi1 mutant that lacks this region is much lower in abundance in comparison to that of native Ddi1 (Figure 2A).

Finally, we found that the phosphorylation of Ddi1 is critical for its function relative to the Sso t-SNAREs. This is because only those forms of Ddi1 that can undergo phosphorylation (e.g., native Ddi1, Ddi1^{S341A}) could facilitate the growth of *sec9-4* cells (Figure 6C), which contain a t-SNARE weakened in its ability to assemble into ternary SNARE complexes. In contrast, mutations that inhibit phosphorylation (e.g., Ddi1^{T346A}, Ddi1^{T348A}), as seen in Figure 6A, had no ability to rescue the growth of *sec9-4* cells at semirestrictive temperatures (Figure 6C). Thus, the rescue of *sec9-4* cells seen upon Sso1 overproduction (which likely facilitates ternary SNARE complex assembly), is mimicked by Ddi1 phosphorylation. How Ddi1 phosphorylation enhances SNARE function is not yet known; however, it may alter the ability of Ddi1 to efficiently inhibit exocytic SNARE complex assembly, as shown earlier by us (Marash and Gerst, 2003).

Many questions remain to be answered regarding the diverse roles of Ddi1 in both regulation of the exocytic machinery and its connection to the cell cycle control through ubiquitin-mediated degradative pathways. We envisage Ddi1 as an intermediary that acts to coordinate both processes, a role suggested previously by us for both protein kinase A and ceramide-activated protein phosphatase functions in cell growth through the control of Sso t-SNARE phosphorylation (Marash and Gerst, 2001).

ACKNOWLEDGMENTS

We thank Tamar Ziv (Smoler Protein Center, Technion, Haifa, Israel) for mass spectrometry analysis and helpful discussion; Jeanne Hirsch (Mount Sinai School of Medicine, NY); Peter Novick (Yale, New Haven, CT), Steven Reed (Scripps Research Institute, La Jolla, CA); and Micah Robinson (Tel Aviv University, Tel Aviv, Israel) for providing reagents. We also thank Deborah Fass and Shmuel Pietrokovski (Weizmann Institute of Science, Rehovot, Israel) for helpful discussions. This work was supported in part by a grant to J.E.G. by the Israel Science Foundation and Y. Leon Benoziyo Institute of Molecular Medicine, Weizmann Institute of Science. J.E.G. holds the Henry Kaplan Chair in Cancer Research.

REFERENCES

Bardin, A. J., and Amon, A. (2001). Men and sin: what's the difference? Nat. Rev. Mol. Cell Biol. *2*, 815–826.

Bernard, D., Mehul, B., Thomas-Collignon, A., Delattre, C., Donovan, M., and Schmidt, R. (2005). Identification and characterization of a novel retroviral-like aspartic protease specifically expressed in human epidermis. J. Invest. Dermatol. *125*, 278–287.

Bertolaet, B. L., Clarke, D. J., Wolff, M., Watson, M. H., Henze, M., Divita, G., and Reed, S. I. (2001a). UBA domains mediate protein-protein interactions between two DNA damage-inducible proteins. J. Mol. Biol. *313*, 955–963.

Bertolaet, B. L., Clarke, D. J., Wolff, M., Watson, M. H., Henze, M., Divita, G., and Reed, S. I. (2001b). UBA domains of DNA damage-inducible proteins interact with ubiquitin. Nat. Struct. Biol. *8*, 417–422.

Biggins, S., Ivanovska, I., and Rose, M. D. (1996). Yeast ubiquitin-like genes are involved in duplication of the microtubule organizing center. J. Cell Biol. *133*, 1331–1346.

Clarke, D. J., Mondesert, G., Segal, M., Bertolaet, B. L., Jensen, S., Wolff, M., Henze, M., and Reed, S. I. (2001). Dosage suppressors of pds1 implicate ubiquitin-associated domains in checkpoint control. Mol. Cell. Biol. *21*, 1997–2007.

Davies, D. R. (1990). The structure and function of the aspartic proteinases. Annu. Rev. Biophys. Biophys. Chem. *19*, 189–215.

Diaz-Martinez, L. A., Kang, Y., Walters, K. J., and Clarke, D. J. (2006). Yeast UBL-UBA proteins have partially redundant functions in cell cycle control. Cell Div. *1*, 28–38.

Elsasser, S., Chandler-Militello, D., Muller, B., Hanna, J., and Finley, D. (2004). Rad23 and Rpn10 serve as alternative ubiquitin receptors for the proteasome. J. Biol. Chem. *279*, 26817–26822.

Elsasser, S., and Finley, D. (2005). Delivery of ubiquitinated substrates to protein-unfolding machines. Nat. Cell Biol. *7*, 742–749.

Gabriely, G., Kama, R., and Gerst, J. E. (2007). Involvement of specific COPI subunits in protein sorting from the late endosome to the vacuole in yeast. Mol. Cell. Biol. *27*, 526–540.

Hartmann-Petersen, R., and Gordon, C. (2004). Integral UBL domain proteins: a family of proteasome interacting proteins. Semin. Cell Dev. Biol. *15*, 247–259.

Hicke, L., Schubert, H. L., and Hill, C. P. (2005). Ubiquitin-binding domains. Nat. Rev. Mol. Cell Biol. *6*, 610–621.

Huh, W. K., Falvo, J. V., Gerke, L. C., Carroll, A. S., Howson, R. W., Weissman, J. S., and O'Shea, E. K. (2003). Global analysis of protein localization in budding yeast. Nature *425*, 686–691.

Ivantsiv, Y., Kaplun, L., Tzirkin-Goldin, R., Shabek, N., and Raveh, D. (2006). Unique role for the UbL-UbA protein Ddi1 in turnover of SCFUfo1 complexes. Mol. Cell. Biol. *26*, 1579–1588.

Kang, Y., Vossler, R. A., Diaz-Martinez, L. A., Winter, N. S., Clarke, D. J., and Walters, K. J. (2006). UBL/UBA ubiquitin receptor proteins bind a common tetraubiquitin chain. J. Mol. Biol. *356*, 1027–1035.

Kaplun, L., Tzirkin, R., Bakhrat, A., Shabek, N., Ivantsiv, Y., and Raveh, D. (2005). The DNA damage-inducible UbL-UbA protein Ddi1 participates in Mec1-mediated degradation of Ho endonuclease. Mol. Cell. Biol. *25*, 5355–5362.

Kim, I., Mi, K., and Rao, H. (2004). Multiple interactions of rad23 suggest a mechanism for ubiquitylated substrate delivery important in proteolysis. Mol. Biol. Cell *15*, 3357–3365.

Krylov, D. M., and Koonin, E. V. (2001). A novel family of predicted retroviral-like aspartyl proteases with a possible key role in eukaryotic cell cycle control. Curr. Biol. *11*, R584–R587.

Lambertson, D., Chen, L., and Madura, K. (1999). Pleiotropic defects caused by loss of the proteasome-interacting factors Rad23 and Rpn10 of *Saccharomyces cerevisiae*. Genetics *153*, 69–79.

Liu, Y., and Xiao, W. (1997). Bidirectional regulation of two DNA-damage-inducible genes, MAG1 and DDI1, from *Saccharomyces cerevisiae*. Mol. Microbiol. *23*, 777–789.

Longtine, M. S., McKenzie, A., 3rd, Demarini, D. J., Shah, N. G., Wach, A., Brachat, A., Philippsen, P., and Pringle, J. R. (1998). Additional modules for versatile and economical PCR-based gene deletion and modification in *Saccharomyces cerevisiae*. Yeast *14*, 953–961.

Lustgarten, V., and Gerst, J. E. (1999). Yeast VSM1 encodes a v-SNARE binding protein that may act as a negative regulator of constitutive exocytosis. Mol. Cell. Biol. *19*, 4480–4494.

Marash, M., and Gerst, J. E. (2001). t-SNARE dephosphorylation promotes SNARE assembly and exocytosis in yeast. EMBO J. *20*, 411–421.

Marash, M., and Gerst, J. E. (2003). Phosphorylation of the autoinhibitory domain of the Sso t-SNAREs promotes binding of the Vsm1 SNARE regulator in yeast. Mol. Biol. Cell *14*, 3114–3125.

Matsui, T., Kinoshita-Ida, Y., Hayashi-Kisumi, F., Hata, M., Matsubara, K., Chiba, M., Katahira-Tayama, S., Morita, K., Miyachi, Y., and Tsukita, S. (2006). Mouse homologue of skin-specific retroviral-like aspartic protease involved in wrinkle formation. J. Biol. Chem. *281*, 27512–27525.

Miller, M., Jaskolski, M., Rao, J. K., Leis, J., and Wlodawer, A. (1989). Crystal structure of a retroviral protease proves relationship to aspartic protease family. Nature *337*, 576–579.

Quimby, B. B., Arnaoutov, A., and Dasso, M. (2005). Ran GTPase regulates Mad2 localization to the nuclear pore complex. Eukaryot. Cell *4*, 274–280.

Rao, H., and Sastry, A. (2002). Recognition of specific ubiquitin conjugates is important for the proteolytic functions of the ubiquitin-associated domain proteins Dsk2 and Rad23. J. Biol. Chem. *277*, 11691–11695.

Rechsteiner, M., and Rogers, S. W. (1996). PEST sequences and regulation by proteolysis. Trends. Biochem. Sci. *21*, 267–271.

Rose, M. D., Winston, F., and Hieter, P. (1990). Methods in Yeast Genetics, Cold Spring Harbor, NY: Cold Spring Harbor Laboratory Press.

Russell, S. J., Steger, K. A., and Johnston, S. A. (1999). Subcellular localization, stoichiometry, and protein levels of 26 S proteasome subunits in yeast. J. Biol. Chem. *274*, 21943–21952.

Saeki, Y., Saitoh, A., Toh-e, A., and Yokosawa, H. (2002). Ubiquitin-like proteins and Rpn10 play cooperative roles in ubiquitin-dependent proteolysis. Biochem. Biophys. Res. Commun. *293*, 986–992.

Sasaki, T., Funakoshi, M., Endicott, J. A., and Kobayashi, H. (2005). Budding yeast Dsk2 protein forms a homodimer via its C-terminal UBA domain. Biochem. Biophys. Res. Commun. *336*, 530–535.

Sirkis, R., Gerst, J. E., and Fass, D. (2006). Ddi1, a eukaryotic protein with the retroviral protease fold. J. Mol. Biol. *364*, 376–387.

Valdez-Taubas, J., and Pelham, H. R. (2003). Slow diffusion of proteins in the yeast plasma membrane allows polarity to be maintained by endocytic cycling. Curr. Biol. *13*, 1636–1640.

Wilkinson, C. R., Seeger, M., Hartmann-Petersen, R., Stone, M., Wallace, M., Semple, C., and Gordon, C. (2001). Proteins containing the UBA domain are able to bind to multi-ubiquitin chains. Nat. Cell Biol. *3*, 939–943.

Wilkinson, C. R., Wallace, M., Morphew, M., Perry, P., Allshire, R., Javerzat, J. P., McIntosh, J. R., and Gordon, C. (1998). Localization of the 26S proteasome during mitosis and meiosis in fission yeast. EMBO J. *17*, 6465–6476.